

### 3D Raman Sideband Cooling of Cesium Atoms at High Density

Dian-Jiun Han, Steffen Wolf, Steven Oliver, Colin McCormick, Marshall T. DePue, and David S. Weiss

*Department of Physics, University of California at Berkeley, Berkeley, California 94720-7300*

(Received 10 January 2000)

We laser cool  $5 \times 10^7$  Cs atoms to a spin-polarized phase space density of  $1/30$ , the highest ever obtained by laser cooling. It is achieved by compression and polarization gradient cooling in a 3D far-off-resonant optical lattice, followed by 3D Raman sideband cooling optimized at a density of  $1.5 \times 10^{12}$  atoms/cm<sup>3</sup>, and adiabatic release. In the lattice, 23% of the sites are occupied, 95% of the atoms are in the lowest energy magnetic sublevel, and 37% are in the lowest 3D vibrational state.

PACS numbers: 32.80.Pj, 32.80.-t, 42.50.Vk

Unity average occupation of 3D far-off-resonant lattice (FORL) sites has recently been achieved [1]. If all of these atoms could be cooled to the 3D vibrational ground state, the phase space density of the system would be at the Bose-Einstein condensation (BEC) point, thus presenting a new and very rapid approach to BEC [2]. Laser cooled samples just short of BEC would be good thermal reservoirs for continuous wave atom lasers [3]. Sufficient cooling of atoms packed tightly in a FORL could allow the study of quantum phase transitions in a periodic potential [4]. Atom interferometry with these atoms would create entangled states that could be the basis for a quantum computer [5,6] or a quantum simulator [7]. The atoms could also be used to study the novel behavior of atom-atom scattering in reduced dimensions [8]. In this Letter, we present significant progress in the laser cooling of atoms in a highly occupied FORL. We produce an optically pumped free space, phase space density that is 6 times higher than any previous laser cooling method.

The previous best reported laser cooled phase space densities were obtained by 1D Raman sideband cooling followed by thermalization [9] and by polarization gradient cooling (PGC) Cs atoms in a 3D FORL [1,10]. In the latter work, atoms were distributed among seven magnetic sublevels, with a phase space density of  $1/190$  in each. Although heating due to rescattered photons severely limits most types of laser cooling, including optical molasses and Raman cooling in dipole traps [11–13], it is not the biggest limitation on PGC in a FORL [10]. In a FORL, this heating is suppressed when the vibrational frequency exceeds the light scattering rate [14]. Tight binding in a FORL also blunts the effect of recoil heating [10]. But the absence in PGC of a vibrational state-selective dark state limits the 3D ground state population to about 30% [1]. To increase the population in a single magnetic sublevel in the vibrational ground state, we have implemented Raman sideband cooling in 3D.

Raman sideband cooling of neutral atoms in FORLs has been demonstrated in 2D [15], 1D [9,16], and very recently in 3D [17]. As population builds up in one magnetic sublevel, heating due to rescattering once again becomes the major barrier to phase space density, albeit at a level about 2 orders of magnitude higher than non-FORL techniques. Our approach to 3D Raman sideband cooling differs from others in 2D and 3D in that it is designed around a FORL that traps all magnetic sublevels identically. This type of FORL does not by itself drive Raman transitions between different sublevels, and so allows the two main steps in the cooling process, stimulated Raman transfer and optical pumping, to be temporally distinct, as in free space Raman cooling [16,18]. They can thus be optimized independently to minimize heating due to rescattering, which makes cooling effective at significantly higher densities. This type of FORL is also implicit in proposed quantum logic schemes [5,6].

We will first describe how this implementation of Raman sideband cooling would work in 1D. Later, in the discussion of the experimental method, we show how we generalize it to 3D. The FORL consists of a  $\pi$ -polarized standing wave. Atoms are trapped in the Lamb-Dicke regime  $k\Delta x \ll 1$ , where  $k$  is the wave number of the FORL light and  $\Delta x$  is the spatial extent of the atomic wave function. Atoms are optically pumped into the lower hyperfine  $m_F = F$  state, which is dark to the optical pumping light. As was originally implemented in Ref. [15], a magnetic field is applied to make the states  $|g, m_F, n\rangle$  and  $|g, m_F - 1, n - 1\rangle$  degenerate, where  $n$  is the vibrational quantum number of the atom in the FORL, and  $g$  is the ground electronic state. Because the FORL light is  $\pi$  polarized, it does not by itself induce stimulated Raman transitions between the degenerate states. We pulse on a Raman beam, which is a  $\sigma$ -polarized traveling wave with the same frequency as the FORL light. The Raman beam works in conjunction with the FORL light to drive these transitions with matrix elements of the form

$$\langle g, F - 1, n - 1 | V_F \hat{\pi} \cos(kx) \left( \sum_e \int_p |e, F - 1, p\rangle \langle e, F - 1, p| \right) V_R \hat{\sigma}^- e^{ikx} |g, F, n\rangle / \delta,$$

where  $V_F$  and  $V_R$  are the electric dipole operators associated with the FORL and Raman beams respectively,  $e$  refers to the relevant excited electronic states,  $p$  refers to the associated unbound motional states, and  $\delta$  is the (far) detuning from the excited states. Because the FORL light has even parity around the trap center, only the Raman beam is responsible for the vibrational energy reducing  $\Delta n = -1$  transitions. When the tightly bound atoms are subsequently optically pumped back to  $m_F = F$ , they are unlikely to change their vibrational state, so the full cycle cools. The cycle is then repeated many times. Atoms accumulate in the lowest energy state,  $|g, F, 0\rangle$ , because it is dark to both the Raman and optical pumping transitions.

The apparatus is similar to that described in Ref. [1]. A cylindrically symmetric distribution of  $9 \times 10^7$  atoms is prepared in a 3D FORL, (see Fig. 1) which is composed of a 1D FORL trap combined with a 2D FORL. The 1D FORL trap is made from a vertically oriented, linearly polarized, retroreflected beam. The 2D FORL consists of two orthogonal, horizontally oriented, vertically polarized standing waves, interferometrically locked to have zero relative phase [1,19]. Each FORL beam has about 300 mW in a  $460 \mu\text{m}$  beam radius, and is detuned 165 GHz to the red of the  $6S_{1/2}, F = 4 \rightarrow 6P_{3/2}$  transitions. The 2D FORL light is frequency shifted by 180 MHz with respect to the 1D FORL light, so that the time-averaged polarization is linear everywhere in the 3D FORL [10]. With the far detuning, this makes the trap depth the same for all magnetic sublevels and prevents the 3D FORL from driving stimulated Raman transitions between magnetic sublevels. The depth at the center of each FORL site is  $160 \mu\text{K}$  vertically, and  $320 \mu\text{K}$  horizontally, but the lattice spatial frequency is  $\sqrt{2}$  greater in the vertical direction, so the vibrational frequency is about the same in all directions,  $\sim 180 \text{ kHz}$ .

We use PGC in two stages to cool the tightly bound atoms to an average energy of  $8.5 \mu\text{K}$  [1]. We measure temperature by taking high intensity fluorescent images of the atoms before and after a 20–30 ms delay [10]. To

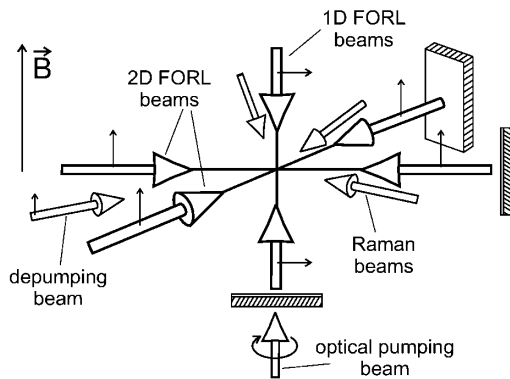


FIG. 1. Experimental setup. The Raman beams and the horizontal FORL beams have the same frequency. All three Raman beams are linearly polarized in the horizontal plane.

duce inhomogeneous broadening of the Raman resonance, and to achieve a higher spatial density, we use the methods of Ref. [1] to spatially compress and then recool the cloud. Compression and recooling is performed first in the vertical and then in the horizontal direction, stopping the free evolution in each case before the peak density is reached. When it is done, the average energy is  $9 \mu\text{K}$  and the peak density is  $1.5 \times 10^{12} \text{ cm}^{-3}$ , which corresponds to a 3D FORL site occupancy of 23%. We could further double the peak density [1], but this distorts the spatial distribution, making temperature measurements problematic. The  $5 \times 10^7$  atoms that remain cannot collide with each other and so suffer negligible losses after this point.

We measure the vibrational frequency,  $\nu$ , at occupied FORL sites by dithering the FORL intensity by 40% for 20 ms and observing the parametric heating at  $2\nu$  [9]. We then tweak the relative intensities of the FORL beams so that the resonance is 350 kHz in all directions, which implies a  $8.4 \mu\text{K} \cdot k_B$  vibrational level spacing. The resonance widths are only 16 and 35 kHz in the vertical and horizontal directions, respectively. A uniform and well-known value of  $\nu$  is crucial in the ultimate determination of the occupation of the vibrational ground state.

Next we spin polarize the sample by optically pumping the atoms to the  $6S_{1/2}, F = 3, m_F = 3$  state. We use a vertical 375 mG bias magnetic field and illuminate the sample for 5 ms with two beams. One is the optical pumping beam, a vertically propagating, circularly polarized traveling wave, locked 150 MHz to the blue of the  $6S_{1/2}, F = 3 \rightarrow 6P_{1/2}, F' = 3$  transition. The other is the depumping beam, a horizontally propagating, vertically polarized traveling wave, locked 30 MHz to the blue of the  $6S_{1/2}, F = 4 \rightarrow 6P_{3/2}, F' = 4$  transition. An additional  $6S_{1/2}, F = 4 \rightarrow 6P_{3/2}, F' = 3$  depumping beam has no effect, probably because rescattered photons empty the potentially dark  $F = 4, m_F = 0$  state. The intensity of the optical pumping and depumping beams are both  $\sim 100 \text{ mW/cm}^2$ . We have varied the detunings and intensities over a wide range to minimize heating while still optically pumping well. Because photon reabsorption depends heavily on these parameters, the heating can vary by more than an order of magnitude for the same quality of optical pumping. Even the optimized spin polarization heats the atoms by  $6 \mu\text{K}$ , 3 times more than we calculate would occur with no rescattering and a completely dark  $6S_{1/2}, F = 3, m_F = 3$  state.

We use three traveling wave Raman beams, each  $\sim 15^\circ$  away from one of the FORL axes (see Fig. 1). A beam for each direction is required because atomic motion near a FORL site center is separable in 3D. The Raman beams are linearly polarized in the horizontal plane and have the same frequency as the 2D FORL light. The 2D FORL always contributes a photon to the Raman transition, but the parity of the FORL light at the trap center prevents those photons from driving  $\Delta n = \pm 1$  transitions. The vertical Raman beam is  $8 \text{ W/cm}^2$  at the FORL, and the horizontal

beams are  $3.5 \text{ W/cm}^2$ . Interferometric measurements show that despite different optical paths, the Raman and FORL beams stay in phase for milliseconds, and so can yield efficient Raman transfer as long as the pulses are much shorter than 1 ms. We use a Blackman pulse shape [20] to minimize off-resonant excitation of  $\Delta n = 0$  transitions, which have a much larger matrix element than the desired  $\Delta n = -1$  transitions, and can undermine the integrity of the Raman-cooled dark state.

The Raman beams cannot all be pulsed on together, because they would interfere and create additional dark states. To Raman cool, we first apply a vertical Raman beam pulse, followed by a square profile optical pumping pulse. We then pulse on the horizontal Raman beams together (for convenience), and optically pump again [21]. The depumping beam is on throughout. The cycle is typically repeated 50 times. At a density of  $1.5 \times 10^{12} \text{ cm}^{-3}$ , we adjust the pulse lengths to minimize the final temperature. An optical pumping pulse length between 75 and  $250 \mu\text{s}$  is optimal, and  $35 \mu\text{s}$  is best for both Raman pulses.

Figure 2 shows the temperature in the horizontal and vertical direction after the FORL is suddenly shut off, as a function of the bias field during Raman cooling. Both temperatures are smallest at 375 mG, which corresponds to a Zeeman splitting of 130 kHz. The minima are shifted by 45 kHz from the measured vibrational splitting, and hence the  $|m_F, n\rangle \rightarrow |m_F - 1, n - 1\rangle$  Raman resonance. We have also observed that, with no Raman beams, the optical pumping heating rate is half as large at 250 mG than at 500 mG. We suspect that the field-dependent heating rate results from FORL polarization impurities that allow weak Raman processes during optical pumping, probably when the atoms are in the  $F = 4$  ground state. The minimum temperature occurs at a bias field between the minimum optical pumping heating and the Raman resonance. The width of the cooling resonance is due to the Blackman pulse width, which is wide enough to excite the  $|m_F, n\rangle \rightarrow |m_F - 1, n - 1\rangle$  transition off resonance.

The horizontal temperature shows another resonance at 900 mG. It is associated with  $|m_F, n\rangle \rightarrow |m_F - 1, n - 2\rangle$  Raman transitions. The cooling resonance coincides with the Raman resonance because the optical pumping heating rate is flat as a function of these larger bias fields. The 2D FORL beams do contribute to these vibrational state changing transitions, because the initial and final states have the same parity. The second feature in the vertical direction is negligible because the 1D FORL beams have a different frequency from the Raman beams and so do not contribute to any Raman process.

Figure 3 shows the final temperature after nonadiabatic shutoff of the FORL as a function of the number of Raman cooling cycles. Within 30 pulses it equilibrates to a horizontal temperature of  $8 \mu\text{K}$  and a vertical temperature of  $7.3 \mu\text{K}$ . By using the parametric heating measurement to determine the zero point energy, we calculate the oc-

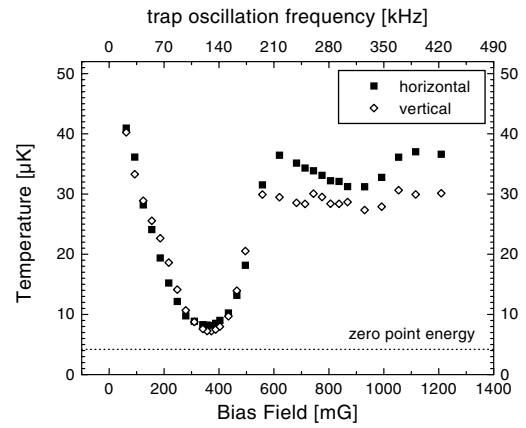


FIG. 2. Temperature after Raman cooling as a function of bias magnetic field. The density is  $1.5 \times 10^{12} \text{ cm}^{-3}$ .

cupation of the vibrational ground state to be 75% in the vertical direction and 70% in horizontal directions, so 37% of the atoms are in the 3D ground state. Cooling takes as little as 4 ms, a negligible part of the experiment's 500 ms repetition time.

To characterize the quality of optical pumping after the Raman cooling cycle we perform a pulsed Stern-Gerlach experiment [22]. We shut off the 3D FORL adiabatically and pulse on an inhomogeneous magnetic field, so that atoms with different magnetic quantum numbers separate before we image them. The  $6S_{1/2}, F = 3, m_F = 3$  state has 95% of the atoms after optical pumping. We also measure the fraction of atoms in the  $6S_{1/2}, F = 4$  state, using an absorption probe resonant with the  $6S_{1/2}, F = 4 \rightarrow 6P_{3/2}, F' = 5$  transition, with and without a repumping beam; it is less than 2%.

We have also measured the final temperature after sudden FORL shutoff as a function of the atomic density, with the size and shape of the atomic distribution constant. Figure 4 shows the temperatures as a function of the peak density. The marginal dependence of temperature on density corresponds to a change in ground state occupation of  $0.05/10^{11} \text{ cm}^{-3}$ . The density dependence is much weaker below  $1.2 \times 10^{12} \text{ cm}^{-3}$ .

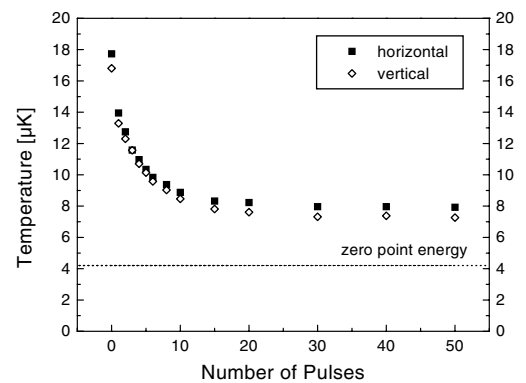


FIG. 3. Temperature as a function of the number of Raman cooling cycles applied. The density is  $1.5 \times 10^{12} \text{ cm}^{-3}$ .

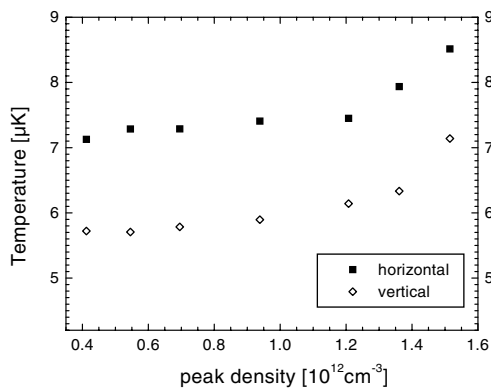


FIG. 4. Temperature as a function of density in the FORL.

Our relative insensitivity to high density comes at the expense of ground state occupation at low density. Detuned optical pumping light is rescattered less, but detuning also makes processes that excite atoms out of the Raman-cooled dark state more important. These processes include off-resonant excitation by the optical pumping light on the  $6S_{1/2}, F = 3 \leftrightarrow 6P_{1/2}, F' = 4$  transition and spontaneous scattering of the FORL light. Although we have not reoptimized all of the cooling parameters at lower density, we checked for such a tradeoff by adjusting the optical pumping laser at  $7 \times 10^{11} \text{ cm}^{-3}$ . When it is tuned on resonance with  $1/8$  the intensity, the final temperatures are  $6.4$  and  $5.3 \mu\text{K}$  in the horizontal and vertical direction respectively, corresponding to a 3D ground state occupation of 56%. In contrast, this optical pumping at  $1.5 \times 10^{12} \text{ cm}^{-3}$  gives a ground state occupation of 26%.

We have adiabatically cooled [23] the atoms by slowly reducing the 3D FORL intensity. With  $1.5 \times 10^{12} \text{ cm}^{-3}$  density, the lowest temperature after adiabatic release from the 3D FORL is  $(250 \pm 30)$  and  $(380 \pm 10)$  nK in the horizontal and vertical directions, respectively. The free space phase space density is  $n_A \lambda_{dB}^3 = 1/30$ , about 15 times higher than the recently reported 3D Raman sideband cooling result [17]. In fact, this understates the quality of our FORL-based cooling, because the adiabatic trap depth reduction extends over only a factor of 1000, so the trap is still several hundred nK deep when it is suddenly extinguished. Theoretical results from Ref. [23] show how to adiabatically transform from our tightly bound periodic structure to free space. Combined with our accurately measured ground state occupation, we infer that perfect adiabatic shutoff would give a phase space density of  $1/16$ .

It is natural to ask what can be done to further improve Raman sideband cooling at high density, especially since some interesting applications require ground state occupations exceeding 85% [7]. Because our best cooling is not at the Raman transition resonance, it would be better to optimize the bias field for the Raman pulses and the optical

pumping separately. Exciting Raman sideband transitions between hyperfine levels would effectively accomplish this [16]. Our relatively worse horizontal cooling probably results from pulsing the horizontal beams on together, which could be avoided. Since the same amount of recoil heating decreases the ground state occupation less when the FORL is deeper, it may be better to use a still deeper FORL.

This work shows that tight binding in a FORL and a flexible approach to laser cooling can address the problem of photon rescattering. There seems to be no intractable barrier to laser-cooled phase space densities of one, even with more than  $10^7$  atoms. If one could optically pump two atoms at a site without collisional loss, BEC could be achieved by laser cooling alone.

In conclusion, we have demonstrated resolved sideband Raman cooling in a 3D FORL. Combined with spatial compression it has produced spin-polarized laser cooled samples with a phase space density of  $1/30$  in free space, the highest of any laser cooling technique to date.

We thank the NSF, the ONR, and the Packard Foundation for their support. S. W. was supported by the Deutsche Forschungsgemeinschaft.

*Note added.*—Recently,  $4 \times 10^4$  Sr atoms have been Doppler cooled to a phase space density of  $1/10$  [24].

- 
- [1] M. DePue *et al.*, Phys. Rev. Lett. **82**, 2262 (1999).
  - [2] M. Anderson *et al.*, Science **269**, 198 (1995).
  - [3] E. Hagley *et al.*, Science **283**, 1706 (1999).
  - [4] D. Jaksch *et al.*, Phys. Rev. Lett. **81**, 3108 (1998).
  - [5] D. Jaksch *et al.*, Phys. Rev. Lett. **82**, 1975 (1999).
  - [6] G. Brennen *et al.*, Phys. Rev. Lett. **82**, 1060 (1999).
  - [7] A. Sørensen and K. Mølmer, Phys. Rev. Lett. **83**, 2274 (1999).
  - [8] M. Olshani, Phys. Rev. Lett. **81**, 938 (1998).
  - [9] V. Vuletic *et al.*, Phys. Rev. Lett. **81**, 5768 (1998).
  - [10] S. Winoto *et al.*, Phys. Rev. A **59**, R19 (1999).
  - [11] D. Boiron *et al.*, Phys. Rev. A **53**, R3734 (1996).
  - [12] H. Perrin *et al.*, Europhys. Lett. **46**, 141 (1999).
  - [13] H. Lee *et al.*, Phys. Rev. Lett. **76**, 2658 (1996).
  - [14] Y. Castin *et al.*, Phys. Rev. Lett. **80**, 5305 (1998).
  - [15] S. Hamann *et al.*, Phys. Rev. Lett. **80**, 4149 (1998).
  - [16] H. Perrin *et al.*, Europhys. Lett. **42**, 395 (1998).
  - [17] A. Kerman *et al.*, Phys. Rev. Lett. **84**, 439 (2000).
  - [18] M. Kasevich and S. Chu, Phys. Rev. Lett. **69**, 1741 (1992).
  - [19] A. Hemmerich *et al.*, Phys. Rev. Lett. **72**, 625 (1994).
  - [20] F. Harris, Proc. IEEE **66**, 51 (1978).
  - [21] Simultaneous application of the two horizontal Raman beams creates a spatial modulation of their net polarization. At sites where their polarization is not linear, the ac Stark shift shifts the Raman resonance. To cool all sites identically, we modulate the phase of one of the horizontal Raman beams with a pair of oscillating Brewster plates.
  - [22] L. Goldner *et al.*, Phys. Rev. Lett. **72**, 997 (1994).
  - [23] A. Kastberg *et al.*, Phys. Rev. Lett. **74**, 1542 (1995).
  - [24] T. Ido *et al.*, Phys. Rev. A **61**, 061403(R) (2000).